# Epithelial contact guidance on well-defined micro- and nanostructured substrates

**Ana I. Teixeira[1], George A. Abrams[2], Paul J. Bertics[3], Christopher J. Murphy[2],[*],[‡] and Paul F. Nealey[1],[*],[‡]**

[1]Department of Chemical Engineering, [2]Department of Surgical Sciences, School of Veterinary Medicine and [3]Department of Biomolecular Chemistry, School of Medicine, University of Wisconsin, Madison, WI 53706, USA

*These authors contributed equally to this work

‡Authors for correspondence (e-mail: nealey@engr.wisc.edu, murphyc@svm.vetmed.wisc.edu)

## Summary

The human corneal basement membrane has a rich felt-like surface topography with feature dimensions between 20 nm and 200 nm. On the basis of these findings, we designed lithographically defined substrates to investigate whether nanotopography is a relevant stimulus for human corneal epithelial cells. We found that cells elongated and aligned along patterns of grooves and ridges with feature dimensions as small as 70 nm, whereas on smooth substrates, cells were mostly round. The percentage of aligned cells was constant on substrate tomographies with lateral dimensions ranging from the nano- to the micronscale, and increased with groove depth. The presence of serum in the culture medium resulted in a larger percentage of cells aligning along the topographic patterns than when no serum was added to the basal medium. When present, actin microfilaments and focal adhesions were aligned along the substrate topographies. The width of the focal adhesions was determined by the width of the ridges in the underlying substrate.

This work documents that biologic length-scale topographic features that model features encountered in the native basement membrane can profoundly affect epithelial cell behavior.

Key words: Cell-substrate interactions, Substrate topography, Grooves and ridges, Contact guidance, Focal adhesions, Nanobiology

## Introduction

Cells receive chemical and physical signals from neighboring cells, the surrounding fluid and extracellular matrices (ECMs). Cells integrate these various stimuli and interpret them to generate appropriate cellular responses. Epithelial cells adhere to specialized ECMs called basement membranes that, in addition to providing physical support, present chemical cues to cells through ligands that specifically bind cell-surface receptors. Basement membranes have a felt-like appearance with pores and fibers of nanoscale dimensions (Abrams et al., 2002; Abrams et al., 2000a; Abrams et al., 2000b; Hironaka et al., 1993; Inoue, 1994; Kubosawa and Kondo, 1994; Merker, 1994; Ruben and Yurchenco, 1994; Shirato et al., 1991; Yamasaki et al., 1994). In particular, the lateral dimensions of the features present on the human corneal basement membrane were reported to range from 22 nm to 191 nm (Abrams et al., 2000b). The nanostructured nature of the basement membrane led to the hypothesis explored in the present study – that nanoscale substrate topography, independent from chemistry, is a relevant stimulus for epithelial cells.

Anisotropic topographic features have been shown to induce many cell types to align and migrate along the direction of the anisotropy, a phenomenon called contact guidance (Flemming et al., 1999). We investigated whether human corneal epithelial cells sense and react to nanoscale substrate topographies by evaluating the cellular responses to anisotropic topographic features with dimensions in the nanometer range. Cell elongation and alignment on grooves and ridges of nanoscale dimensions was compared with the morphology and orientation of cells cultured on smooth substrates and on substrates with micrometer-sized grooves and ridges. The smallest topographic features tested (70 nm) were more than 100 times smaller than the width of a single cell. The substrates had uniform surface chemistry, ensuring that chemical anisotropies did not contribute to the observed cellular responses.

Various cell types display contact guidance when cultured on groove and ridge patterns with lateral dimensions in the micrometer range (Clark et al., 1990; den Braber et al., 1995; den Braber et al., 1996a; den Braber et al., 1996b; den Braber et al., 1998; Flemming et al., 1999; Matsuzaka et al., 2000; van Kooten et al., 1998; Walboomers et al., 1999a; Walboomers et al., 1999b; Wojciak-Stothard et al., 1995b; Wojciak-Stothard et al., 1996). Profound differences in cytoskeletal organization have been found between cells elongated and aligned along these topographic features and cells cultured on smooth surfaces. Focal adhesions are adhesive structures containing aggregates of transmembrane proteins called integrins that link the actin cytoskeleton to extracellular matrix proteins. Focal adhesions and actin microfilament bundles (Britland et al., 1996; den Braber et al., 1998; Matsuzaka et al., 2000; Meyle et al., 1994; Walboomers et al., 1998) and microtubules (Oakley and Brunette, 1995a; Oakley et al., 1997) have all been found to align along micrometer-sized grooves and ridges, in cells aligned along these topographic features. On smooth substrates, cells and cytoskeletal elements did not display any preferred orientations.

The sequence of cytoskeletal events and the relative

importance of the actin and microtubule systems in the mechanism of contact guidance remain unclear. Oakley and Brunette (Oakley and Brunette, 1993) proposed that the first event in the reaction of cells to grooves and ridges is the alignment of microtubules, 20 minutes after cell plating. However, the detection of actin condensations along the groove/ridge boundaries 5 minutes after cell adhesion suggested that actin aggregation rather than microtubule alignment is the first and primary event in the contact guidance mechanism (Wojciak-Stothard et al., 1995a). Nonetheless, contact guidance was observed in cells cultured on micrometer-wide grooves and ridges where either the microtubule or the microfilament (Oakley and Brunette, 1995b; Oakley et al., 1997; Walboomers et al., 2000; Wojciak-Stothard et al., 1995a) systems were disrupted by cytoskeletal poisons. Interestingly, when submicrometer features were investigated (500 nm wide grooves and ridges), functional microtubules were found to be necessary to induce contact guidance (Oakley et al., 1997).

Focal adhesion formation and alignment has been proposed to play an important role in the mechanism of contact guidance. Cell and cytoskeletal alignment has generally been found to be more pronounced on patterns with ridge widths between 1 and 5 μm than on grooves and ridges with larger lateral dimensions (den Braber et al., 1995; den Braber et al., 1996a; den Braber et al., 1996b; den Braber et al., 1998; Matsuzaka et al., 2000; Meyle et al., 1994). Moreover, on the narrower features, focal adhesions were almost exclusively located on the tops of the ridges and were aligned along these substrate features. O'Hara and Buck (Ohara and Buck, 1979) proposed that on closely spaced grooves and ridges focal adhesion formation is constrained to the top of the ridges because cell membrane stiffness leads to the bridging of the grooves. Oblong focal adhesions 1-10 μm long (Riveline et al., 2001) orient along the direction of the ridges to maximize their contact area, leading to an alignment of microfilament bundles and of the cell body as a whole (den Braber et al., 1996b; den Braber et al., 1998; Meyle et al., 1994). This explanation has been questioned on the basis of observations that focal adhesions can bend around groove/ridge boundaries (Walboomers et al., 1998).

Nonuniformities in protein deposition on surfaces with anisotropic topographies have also been proposed to play a role in contact guidance (den Braber et al., 1998; von Recum and van Kooten, 1995). According to this hypothesis, the topographic discontinuities have different surface energy and act as sites of preferred protein deposition, creating patterns of proteins along the topographic patterns. Walboomers and colleagues have not found a preference for focal adhesion formation along the groove/ridge boundaries (Walboomers et al., 1998), suggesting that adhesive proteins do not colocalize preferentially with the surface discontinuities. Furthermore, cells have been shown to exhibit contact guidance when cultured on anisotropic substrates without sharp discontinuities (Walboomers et al., 1999a). Although there is no conclusive evidence that the topographic features affect passive deposition of proteins, the assembly of fibronectin (Fn) and vitronectin (Vn) filaments by fibroblasts has been reported to occur along the substrate features (den Braber et al., 1998). These filaments coaligned with actin microfilaments and were able to span grooves and ridges. Substrate discontinuities have also been proposed to cause cell alignment through mechanical

interactions with the cell membrane that induce actin and vinculin condensations along the groove/ridge edge (Wojciak-Stothard et al., 1996; Wojciak-Stothard et al., 1995a; Wojciak-Stothard et al., 1995b).

There are a few reports of contact guidance on submicrometer features; most notably, Clark and colleagues (Clark et al., 1991) found that fibroblast and epithelial cell lines aligned along grooves and ridges 130 nm wide. Similar substrates were found to induce alignment of oligodendrocytes but not of rat hippocampal or cerebellar neurons (Webb et al., 1995).

In the present study we have found that ridges 70 nm wide induced human corneal epithelial cells to elongate and align along the topographic features. This is the smallest feature size that has been reported to induce contact guidance. The percentage of aligned cells was similar for feature pitches ranging from 400 nm (70 nm wide ridges) to 2 μm, but increased with groove depth. Cells on smooth substrates were mostly round, as were those cells on the patterned substrates that were not elongated and aligned along the grooves and ridges. Additionally, the presence of serum in the culture medium increased the percentage of aligned cells, indicating that topography can act synergistically with other cellular inputs.

The range of ridge widths included in the present study (from 70 nm to 1900 nm) encompasses the reported lateral dimensions of the focal adhesions (between 250 nm and 500 nm) (Ohara and Buck, 1979). Therefore, the morphology of focal adhesions on these groove and ridge patterns can be used as an indicator of the threshold in topographic lateral dimensions where cell responses to nanotopographies differ from those to topographic features of larger dimensions. Mature focal adhesions and stress fibers were observed only sporadically. The observation of cells elongated and aligned along the topographic features without focal adhesions and associated stress fibers suggests that assembly of these structures is not necessary in the mechanism of contact guidance of epithelial cells. When focal adhesions were observed, the width of the focal adhesions was controlled by the width of the ridges on the underlying substrate. Focal adhesions in cells cultured on substrates with ridge widths of biomimetic dimensions (70 nm) had significantly smaller widths than focal adhesions in cells cultured on substrates with wider ridges or on smooth substrates. This altered focal adhesion architecture on the nanostructured substrates may have implications in focal adhesion properties such as the tension applied on the substrate or the intracellular signaling cascades generated.

We have established that human corneal epithelial cells are responsive to topographical cues of nanoscale dimensions. Nanoscale substrate topography is therefore a cellular input and may be instrumental in obtaining desired cell behaviors, when presented in context with other inputs. Our findings may have an impact on the design of systems for cell culture, tissue engineering and the development of implantable prosthetics.

## Materials and Methods

### Fabrication of micro- and nanostructured substrates

Four-inch silicon wafers were primed with hexamethyldisilazane in a vacuum oven (Yield Engineering Systems, San Jose, CA) and coated with UV3 photoresist (Shipley, Malborough, MA) in a resist spinner

(Solitec Wafer Processing, San Jose, CA). The resulting resist films were approximately 425 nm thick, measured using an Alpha Step 200 profilometer. The coated wafers were then baked on a vacuum hotplate at 130°C for 60 seconds. The photoresist was patterned in a Cambridge Leica EBMF 10.5 electron-beam lithography tool (Center for Nanotechnology, University of Wisconsin-Madison, WI). The dose applied varied between 16 and 23 $\mu C/cm^2$, depending on the width of the areas exposed to the electron beam to create the different pattern features. The wafers were then baked again for 90 seconds at 130°C. The dissolution of the exposed areas of the resist in a developing solution (MF320, Shipley) created topographic patterns of resist on the wafer.

These resist patterns were transferred to the underlying silicon in a helicon etching tool (Center for Plasma Aided Manufacturing, University of Wisconsin-Madison). The resist acted as a mask, allowing only the exposed silicon areas to be etched. The gases used were $SF_6$ and $C_2H_2F_4$, both with flow rates of 18 sccm. The pressure was 2 mTorr and the antenna power was 1.5 kW. The power applied to the wafer chuck was 15 W, resulting in a bias voltage of –35 V. The antenna discharge, as well as the wafer chuck power, was pulsed at a frequency of 33.3 kHz with 50% duty cycle.

The resist remaining after etching was removed by immersing the wafers in piranha solution (7/3 (v/v) of 98% $H_2SO_4$/30% $H_2O_2$) at 110°C for 30 minutes. The wafers were then copiously rinsed with deionized water. The native silicon oxide layer on the wafers was removed by dipping the wafers in buffered oxide etch (BOE, Arch Chemicals, Norwalk, CT). Following this treatment, the wafers were coated with a layer of silicon oxide in a low pressure chemical vapor deposition reactor (LPCVD, University of Wisconsin-Madison). Oxygen and tetraethylorthosilicate were the gases used; the pressure was 1 Torr and the temperature was 675°C. When samples were re-used, they were first cleaned with piranha solution as described above. The silicon oxide coating was removed by treating the substrates with BOE. The substrates were then re-coated with silicon oxide in the LPCVD reactor.

The patterned wafers were cut with a diamond saw (MicroAutomation 1006, Woodcliff Lake, NJ) into chips containing patterned fields separated by smooth areas. These chips were glued to the bottom of 24-well plates (Becton Dickson, Franklin Lakes, NJ) using silicone aquarium sealant (Perfecto Manufacturing, Noblesville, IN). They were allowed to dry in a laminar flow hood for at least 24 hours and were immersed in deionized water for an additional 24 hours. The samples were then rinsed three times for 10 minutes with deionized water and sterilized by immersing in ethanol for 30 minutes and air-drying in a hood. Finally, they were rinsed three times with sterile PBS for 10 minutes.

## Cell culture

Human corneal epithelial cells were harvested from corneas donated by the Lions Eye Bank of Wisconsin (Madison, WI) or the Missouri Lions Eye Bank (Columbia, MO). The corneal buttons were trimmed to exclude any scleral or limbal regions. The buttons were immersed in a dispase solution (1.2 units/ml, Boehringer Mannheim, Germany) and placed in an incubator for 4 hours. The epithelial cells became loosely adherent and could be removed by gently rubbing the corneas with a pipette tip. The resulting cell suspension was centrifuged and the cells were re-suspended in Epilife[TM] basal medium (Cascade Biologics, Portland, OR) with a growth supplement of defined composition. The growth supplement contained purified bovine serum albumin, purified bovine transferrin, hydrocortisone, recombinant human insulin-like growth factor type-1, prostaglandin and recombinant human epidermal growth factor (EDGS, Cascade Biologics). This cell suspension was transferred to T25 cell culture flasks (Becton Dickson), previously coated with a mixture of fibronectin, collagen and albumin in a buffer (FNC coating mix, Biological Research Faculty and Facility, Inc., Ijamsville, MD). Each

flask contained cells from two to four corneas. The cells were incubated at 37°C and 5% $CO_2$ and were harvested using 0.025% trypsin/0.01% EDTA (Cascade Biologics), after reaching approximately 80% confluency. Neutralization was done with a phosphate-buffered saline solution containing 0.025% purified soybean trypsin inhibitor (Cascade Biologics). Cells were centrifuged and resuspended in a 1:1 mixture of Dulbecco's modified Eagle medium and nutrient mixture F-12 (D-MEM/F-12, Invitrogen, Carlsband, CA) with 0.5% dimethyl sulfoxide (Sigma Chemical Co.). This basal medium was supplemented or not with 10% (v/v) of fetal bovine serum (FBS, Sigma Chemical Co.). Next, cells were plated at a density of 8500 cells/cm$^2$ in 24-well plates containing the patterned silicon chips. They were incubated at 37°C and 5% $CO_2$, for 12 hours.

The medium was removed at the end of the incubation time and the cells rinsed with Dulbecco's phosphate-buffered saline (DPBS) (BioWhitaker, Walkersville, MD). The cells were fixed in 4% paraformaldeyde (Electron Microscopy Sciences, Washington, PA), 5% sucrose in 10 mM phosphate buffer at a pH of 7.4 and at room temperature, for 20 minutes. The cells were then permeabilized with 0.1% Triton X-100 in DPBS for 5 minutes and immersed in 1% bovine serum albumin in DPBS for 20 minutes. Next, the cells were incubated with 5 $\mu g/ml$ of TRITC-phalloidin (Sigma Chemical Co.) in DPBS for 30 minutes. TRITC-phalloidin stains filamentous actin, and we found that we could obtain an accurate representation of the cell outline with this stain, as confirmed by using simultaneously a cell membrane stain such as thiosemicarbazide (Molecular Probes, Eugene, OR). Next, the cells were immersed three times in DPBS for 10 minutes. Cell nuclei were then stained using 90 nM of DAPI (Molecular Probes) in DPBS for 10 minutes followed by rinsing again three times in DPBS. Finally, the substrates were glued onto glass slides and Prolong (Molecular Probes) mounting medium was added to the cell side of the substrates before covering them with glass coverslips.

Vinculin staining was used as a marker for focal adhesions. After staining F-actin as described above, cells were incubated with mouse anti-human vinculin antibody (Sigma Chemical Co.) for 45 minutes at 37°C. The secondary antibody used was donkey anti-mouse immunoglobulin G (Jackson ImmunoResearch Laboratories, West Grove, PA).

## Quantification of cell shape and orientation

The morphology of human corneal epithelial cells cultured on patterned substrates was assessed by analyzing the shapes of all cells adhering to a 1.03×1.30 mm$^2$ region in the center of each of the patterned fields. A similar region was also analyzed on a smooth area of the same sample. Images of the stained cells were obtained from an epifluorescence microscope (Nikon TE300, Melville, NY) with an objective magnification of 20×, and montages of 2×2 images were created. Additionally, images were also obtained of cells that had adhered to the bottom of the 24-well plates (Tissue Culture Polystyrene, TCPS). All images were converted to binary images using Metamorph[TM] software (Universal Imaging Corporation, Downingtown, PA). The area and perimeter of all cells in the images were then automatically measured. The length of the cells, defined as their longest cord, and the cell breadth, the longest chord perpendicular to the length, were also obtained from Methamorph[TM]. Cell elongation was defined as the ratio between the length and breadth of each cell. The angles between the length of the cells and the patterns were also obtained. The cells were considered aligned with the grooves when this angle was less than 10°. The DAPI images assisted in determining whether cells formed clumps or were isolated. All cells in contact with other cells were manually removed from the data sets. All experiments were repeated and ten samples were used in each trial. This resulted in the analysis of over 600 cells for each of the pattern dimensions and culture conditions.

Images of cells stained for vinculin were acquired at a magnification of 100×. Between 40 and 50 focal adhesions of cells

### Table 1. Feature dimensions of the topographically patterned substrates

| Pitch (nm) | Ridge width (nm) | Groove width (nm) |
|---|---|---|
| 400 | 70 | 330 |
| 800 | 250 | 550 |
| 1200 | 400 | 800 |
| 1600 | 650 | 950 |
| 2000 | 850 | 1150 |
| 4000 | 1900 | 2100 |

The groove depth was either 600 nm or 150 nm.

cultured on each of the substrate topographies and on the smooth surfaces were manually traced and analyzed using NIH Image J software.

## Time-lapse microscopy

Cells were seeded on the silicon substrates and incubated for 2 hours at 37°C and 5% $CO_2$. The substrates with adherent cells were then placed on glass coverslip shims set in a glass-bottom dish filled with medium, with the cell side facing down. Images were acquired in an inverted microscope (Zeiss Axiovert 200M) every 30 minutes until 12 hours had elapsed since the cells had been seeded. Four 0.65×0.55 mm$^2$ fields (magnification 20×) were sequentially imaged on patterns of grooves and ridges on a 400 nm pitch and on smooth substrates. All the cells not in contact with other cells (28 cells on 400 nm pitch patterns and 19 cells on smooth silicon substrates) were then manually traced and measured using Image J software.

## Imaging of cell morphology using scanning electron microscopy

Human corneal epithelial cells were rinsed in 0.1 M cacodylate buffer for 10 minutes and fixed in 3% glutaraldehyde in cacodylate buffer (Tousimis, Rockville, MD) for 2.5 hours. The cells were then rinsed in cacodylate buffer and post-fixed in 1% osmium tetroxide for 1 hour (Tousimis). Next, the cells incubated in 1% tannic acid and rinsed in cacodylate buffer. Finally, cells were dehydrated in graded ethanols, immersed in hexamethyldsilazane for 10 minutes, coated with 2 nm of platinum and imaged in a Leo 1530 field emission scanning electron microsope (Leo Electron Microscopy, Thornwood, NY) (Dalton et al., 2001a). Cells were qualitatively examined for overall cell shape, orientation relative to the underlying grooves and ridges and for the presence and morphology of filopodia and lamellipodia.

## Results

### Substrate design

Each substrate consisted of an array of six 4 mm$^2$ fields patterned with grooves and ridges. The feature pitches (sum of the groove and ridge widths) were uniform in each field and ranged from 400 to 4000 nm in the different fields (pitches equal to 400 nm, 800 nm, 1200 nm, 1600 nm, 2000 nm and 4000 nm), in each sample. The relative groove and ridge widths, for a given pitch, were determined by the processing conditions selected. To explore the biomimetic sub-100 nm feature dimensions, we fabricated 70 nm wide ridges on a 400 nm pitch through cumulative reductions in ridge width in the exposure, development and etching steps. The depth of the grooves was either 150 nm or 600 nm (Table 1). The smooth areas between the patterned fields acted as internal controls in
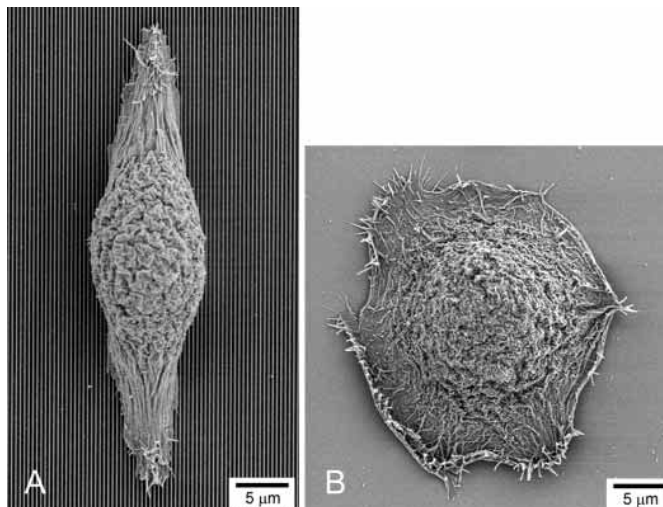


**Fig. 1.** SEM images of human corneal epithelial cells. (A) Cell cultured on a silicon oxide substrate patterned with 70 nm wide ridges, on a 400 nm pitch. The groove depth was 600 nm. (B) Cell on a smooth silicon oxide substrate.

each substrate (Smooth SiOx). We have ensured uniform surface chemistry by conformally coating the substrates with a layer of silicon oxide.

### Human corneal epithelial cells elongate and align along 70 nm wide ridges

A subpopulation of the human corneal epithelial cells cultured on substrates patterned with 70 nm wide ridges and 600 nm deep grooves, on a 400 nm pitch, were elongated and aligned along the direction of the patterns, 12 hours after cell seeding (Fig. 1a). By contrast, cells cultured on the smooth substrates were mostly round (Fig. 1b). The angle between the longest chord in a cell and the direction of the patterns was designated as the cell orientation angle. Cells were considered to be aligned with the substrate patterns when the cell orientation angle was less than 10° (Clark et al., 1990). Approximately 35% of the cells cultured on substrates with 70 nm wide ridges and 600 nm deep grooves, on a 400 nm pitch, were aligned with the substrate topographies. On smooth substrates (SiOx and TCPS), the distribution of cell orientation angles was uniform, indicating that cells were randomly oriented (Fig. 2).

Cells were either elongated and aligned with the grooves and ridges or were approximately round. We defined cell elongation as the ratio between the longest chord in the cell (length) and the longest chord perpendicular to it (breadth). There was no correlation between cell elongation and cell orientation angle for cells cultured on smooth SiOx and TCPS as cells had an almost round morphology (average elongation approximately 1.3). The average elongation of nonaligned cells on patterned substrates (cells with orientation angles between 10° and 90°) was equivalent to the average elongation of cells cultured on smooth substrates. By contrast, aligned cells were on average significantly more elongated than nonaligned cells cultured on the patterned substrates or cells cultured on smooth substrates (Fig. 3).
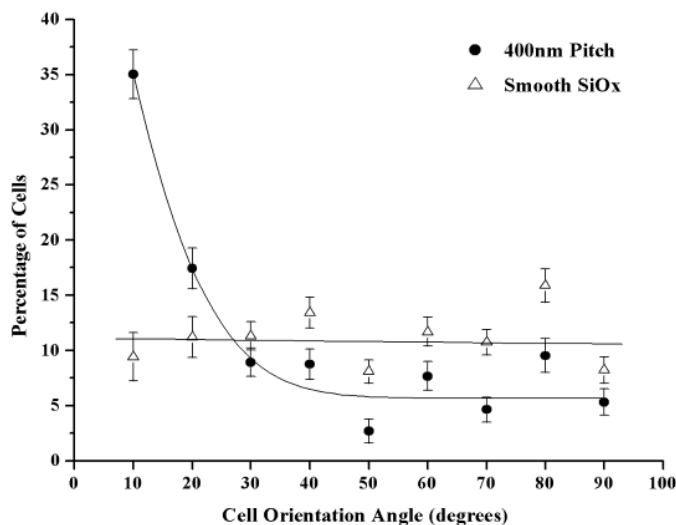
**Fig. 2.** Distribution of orientation angles for cells cultured on substrates patterned with 70 nm wide ridges and 600 nm deep grooves, on a 400 nm pitch (circles), and for cells cultured on smooth silicon oxide substrates (triangles). Each data point corresponds to the percentage of cells that have orientation angles in the 10° angle interval up to the coordinate in the x-axis.
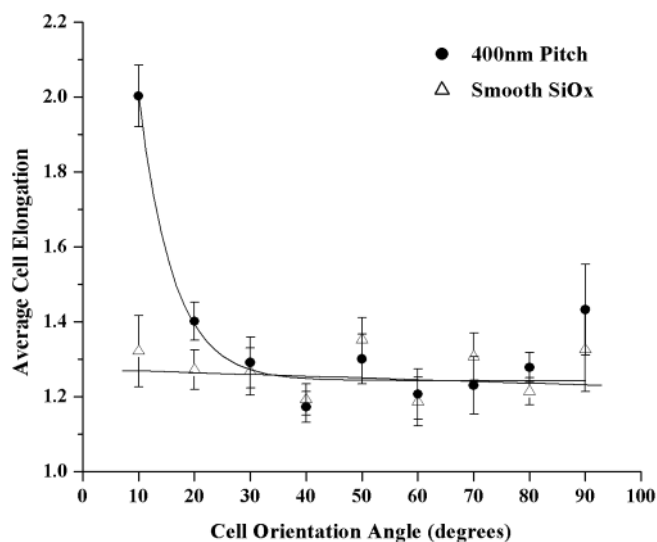


**Fig. 3.** Average cell elongations (cell length/cell breadth) of cells cultured on substrates patterned with 70 nm wide ridges and 600 nm deep grooves, on a 400 nm pitch (circles) and of cells on smooth substrates (triangles). Average elongation of nonaligned cells on patterned substrates (cells with orientation angles between 10° and 90°) was equivalent to the average elongation of cells cultured on smooth substrates. Cells with orientation angles less than 10° were on average significantly more elongated than nonaligned cells cultured on the patterned substrates or cells cultured on smooth substrates.

Therefore, cell elongation correlated strongly with cell alignment on the patterned substrates, where more than 80% of the cells that were considerably elongated (elongation higher than 2) were also aligned along the substrate patterns (Fig. 4).
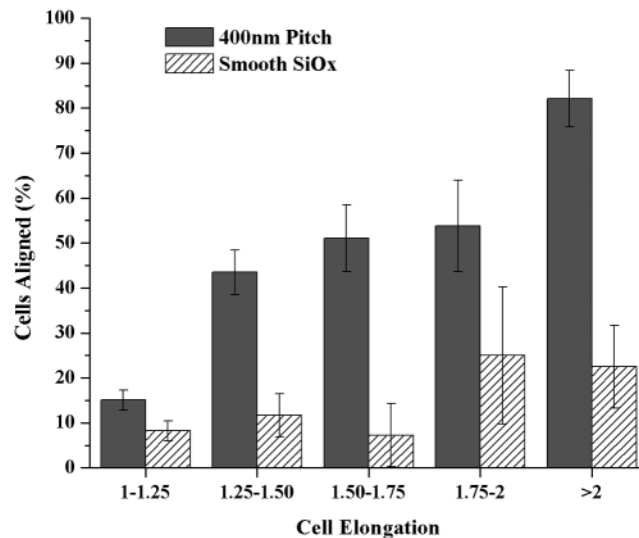


**Fig. 4.** Histogram of cell elongations for cells cultured on substrates patterned with 70 nm wide ridges and 600 nm deep grooves, on a 400 nm pitch and for cells cultured on smooth silicon oxide substrates. On the patterned substrates more than 80% of the cells with elongations higher than 2 were aligned along the substrate patterns. There was no correlation between cell elongation and the percentage of cells with orientation angles less than 10° on the smooth substrates.

## Cells extend and retract lamellipodia along the direction of the patterns

On substrates patterned with grooves and ridges on a 400 nm pitch, cells periodically extended and retracted lamellipodia along the direction of the patterns, as observed with time-lapse microscopy (Fig. 5). Although lamellipodia protruded preferentially along the pattern direction, protrusions perpendicular to the patterns were not prohibited. Cells sometimes acquired a round morphology after retraction of lamellipodia. Furthermore, there was a subpopulation of cells that did not spread and remained round. On smooth substrates, lamellipodial protrusions had random orientations and cells were mostly round.

The centroids of cells cultured on the patterned substrates remained largely stationary for 12 hours after cell seeding (Fig. 6a). Cell trajectories during this time were longer on the smooth than on the patterned substrates (Fig. 6b). The mean square displacement on the smooth substrates was approximately four times larger than on the patterned substrates.

Cells appeared rounded up 2 hours after seeding, on the patterned substrates. On the smooth substrates, many cells had started to spread by this time and the average cell area was larger than on the patterned substrates. Average cell areas remained larger on the smooth than on the patterned substrates, for the duration of the experiment.

## Pattern-induced alignment of corneal epithelial cells is more affected by groove depth than pattern pitch

On substrates with 600 nm deep grooves, the percentage of aligned cells after 12 hours of incubation was constant on patterns with pitches ranging from 400 nm to 2000 nm. A drop

**Fig. 5.** Cells extended and retracted lamellipodia along the direction of the patterns. (A-D) Time-lapse microscopy of a cell cultured on grooves and ridges on a 400 nm pitch. The direction of the patterns can be clearly seen but, due to the resolution of these images, the observed pitch is not correct. (E-H) Cell on smooth silicon oxide. (A,E) 2.5 hours; (B,F) 9.5 hours; (C,G) 10.5 hours; (D,H) 12 hours after cell seeding.
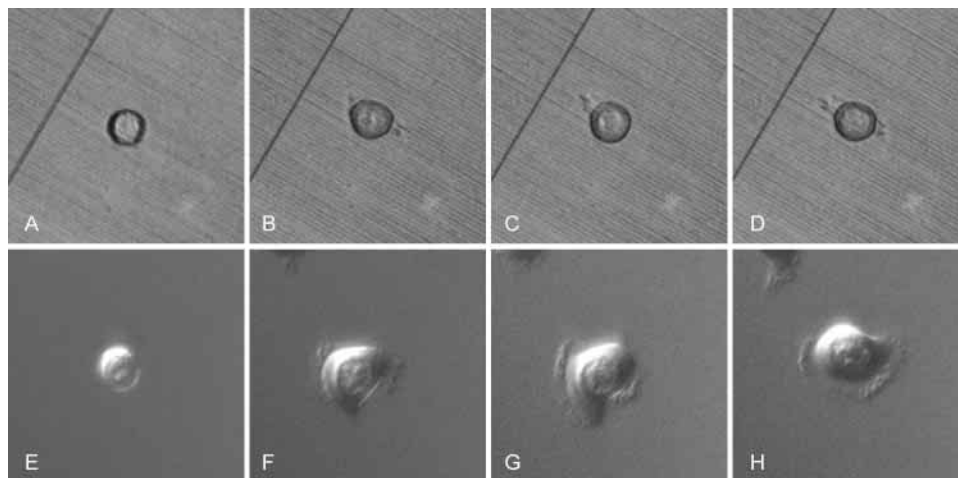


**Fig. 6.** Cells on smooth substrates had longer trajectories than cells on substrates with grooves and ridges on a 400 nm pitch. Cell trajectories correspond to the coordinates of the cells' centroids, recorded every 30 minutes from 2 hours until 12 hours after seeding. The units of the axes are micrometers. (A) The centroids of cells on patterned substrates were mostly stationary. (B) On smooth substrates cells had random trajectories.
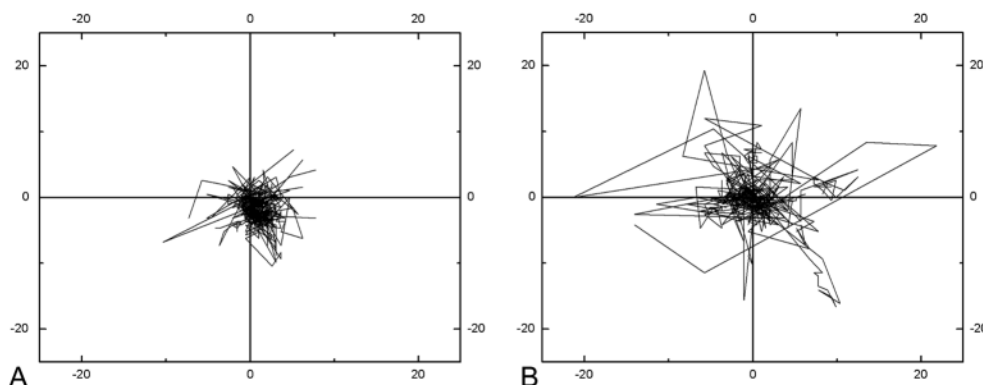
off in cell alignment was observed for the largest pattern pitches (4000 nm). On 150 nm deep grooves, cell alignment was independent of pattern pitch. The percentage of aligned cells was significantly lower on 150 nm than on 600 nm deep grooves, for pitches up to 2000 nm (Fig. 7). On the smooth surfaces (SiOx and TCPS), the distributions of cell orientation angles were consistent with randomly oriented populations of
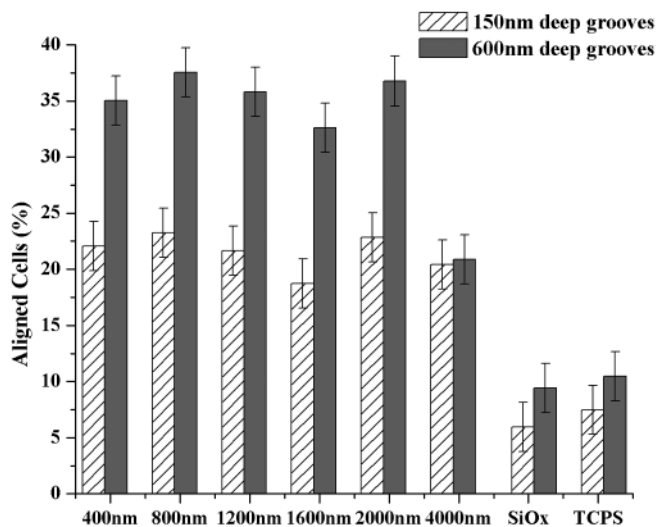
cells, as described above. On substrates with both 150 nm and 600 nm deep grooves, the average elongation of nonaligned cells was similar to the average elongation of cells on the smooth substrates. On 600 nm deep grooves, for all pitches tested, cells that were aligned along the topographic features had higher elongations on average than cells on smooth surfaces. However, on 150 nm deep grooves the average elongations of aligned cells and of cells on smooth surfaces were not statistically different. This is consistent with the reduced number of elongated cells found on the shallower surfaces.

The average area of elongated cells (elongation higher than 1.3) was higher than the area of round cells (elongation lower than 1.3) on both 600 nm and 150 nm deep grooves, for all pattern pitches. The average areas of both elongated and round cells on any of the patterned surfaces were lower than on the smooth surfaces. Moreover, cell areas on TCPS were higher than on smooth SiOx (Fig. 8).



**Fig. 7.** Percentage of cells cultured on patterned and smooth substrates that had orientation angles less than 10° (designated aligned cells). On substrates with 600 nm deep grooves, the percentage of aligned cells was constant on patterns with pitches ranging from 400 nm to 2000 nm and decreased on 4000 nm pitch patterns. On 150 nm deep grooves, cell alignment was equivalent on all pattern pitches and was significantly lower than on 600 nm deep grooves, for pitches up to 2000 nm.
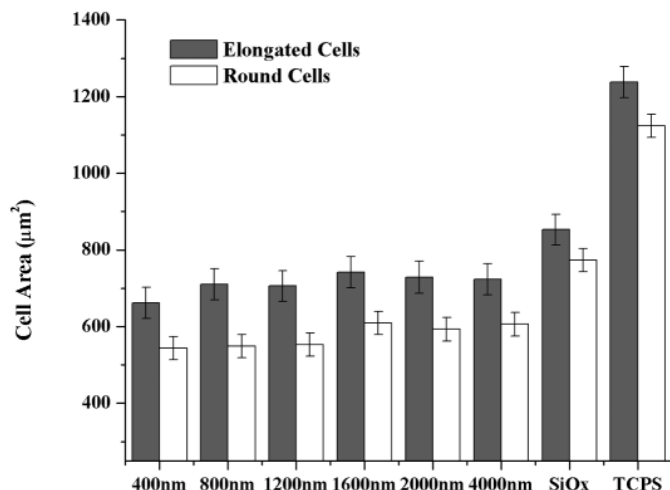
**Fig. 8.** Average projected cell areas of elongated cells (cell elongations higher than 1.3) and round cells (cell elongations lower than 1.3) on substrates patterned with 600 nm deep grooves and pitches between 400 nm and 4000 nm and on smooth substrates (SiOx and TCPS). The culture medium was SHEM with 10% FBS. The average projected cell areas of both elongated and round cells on any of the patterned surfaces were lower than on the smooth surfaces.
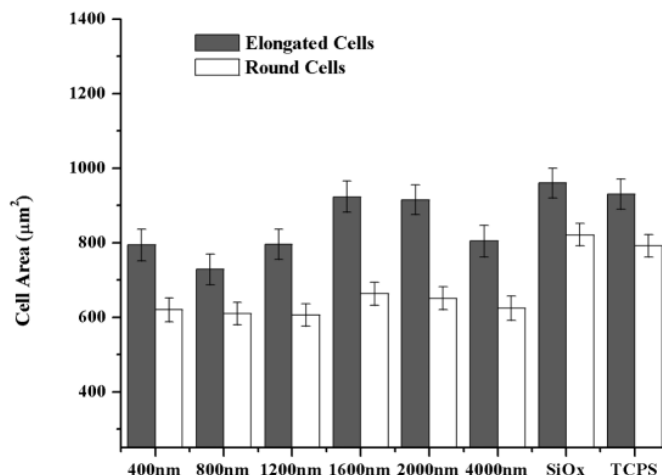


**Fig. 10.** Average projected cell areas of elongated cells (cell elongations higher than 1.3) and round cells (cell elongations lower than 1.3) on substrates patterned with 600 nm deep grooves and pitches between 400 nm and 4000 nm and on smooth substrates (SiOx and TCPS). The culture medium was SHEM and no FBS was added. The average projected cell areas were similar on SiOx and on TCPS.
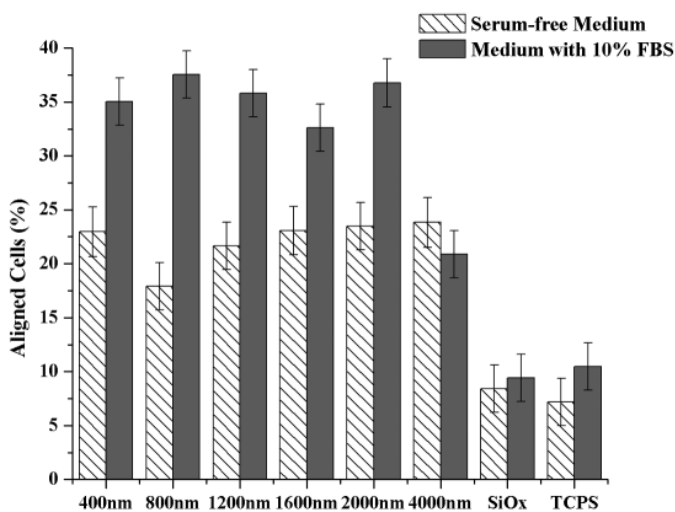


**Fig. 9.** Percentage of aligned cells in the presence or absence of FBS. When FBS was not added to the culture medium the percentage of aligned cells was equivalent on all pattern pitches and was significantly lower than in the presence of serum, for pitches up to 2000 nm.

## Effects of serum in the culture medium

The absence of serum in the culture medium resulted in lower levels of corneal epithelial cell alignment compared with when the medium was supplemented with 10% FBS, on surfaces with equivalent pattern dimensions, on 600 nm deep grooves (Fig. 9). The pitch of the patterns did not affect the percentage of aligned cells. Aligned cells were more elongated on average than cells on smooth surfaces, on all pattern pitches. Elongated cells had larger areas than round cells on all surfaces. Interestingly, cells grown in the absence of serum had the same surface area on smooth silicon as on TCPS, contrary to what

was observed when serum was present in the culture medium (Fig. 10).

## Distribution of filopodia and lamellipodia is affected by substrate topography

Scanning electron microscopy (SEM) revealed that cells were covered with numerous microvilli and formed both lamellipodia and filopodia. On all the patterns tested, filopodia were able to adhere to both grooves and ridges. The topographic features frequently guided the filopodial orientation (Fig. 11). Lamellipodia descended into the grooves at the cell edge along the topographic features, on both narrow (330 nm) and wide (2100 nm) grooves. At the cell edges perpendicular to the patterns, lamellipodia were able to adhere to the floor of the grooves that were 2100 nm wide but not 330 nm wide, on both 150 nm and 600 nm deep grooves (Fig. 12). On 2100 nm wide and 150 nm deep grooves, lamellipodia were frequently observed to conform to the topographic features.

## The width of focal adhesions is controlled by the ridge width

Mature focal adhesions and stress fibers were observed only sporadically in cells cultured on both patterned and smooth substrates. Focal adhesions were observed in cells cultured in DMEM/F12 medium with or without serum. Cells cultured on smooth silicon formed focal adhesions and stress fibers with no preferred orientations. On the patterned substrates focal adhesions and stress fibers aligned along the topographic features (Fig. 13). The measured width of the focal adhesions was dictated by the width of the ridges on the underlying substrate. Focal adhesions formed in cells cultured on substrates with 70 nm wide ridges were significantly narrower than focal adhesions in cells cultured on substrates with ridge widths of more than 400 nm. On substrates with 250 nm wide
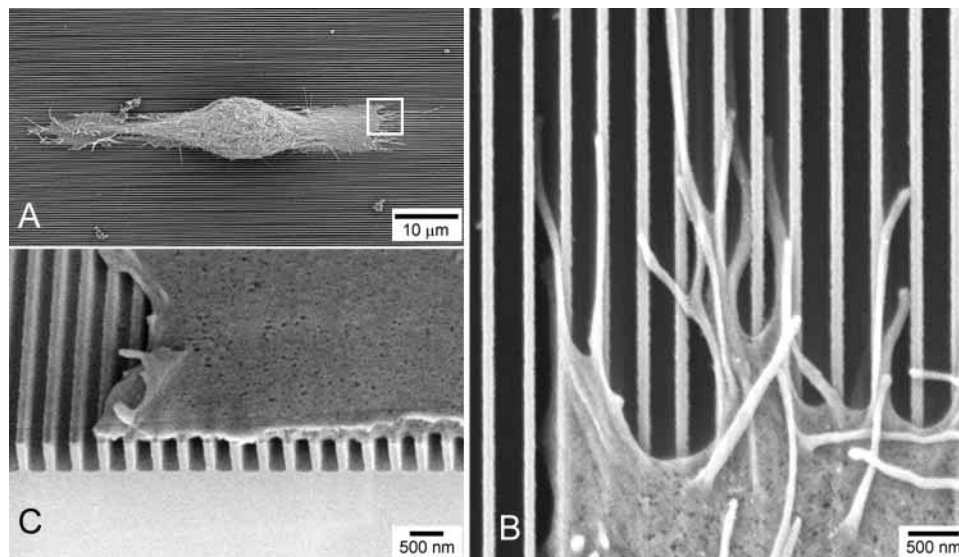
**Fig. 11.** SEM images of cells cultured on patterns with 400 nm pitch. (A) Cell aligned along nanostructured substrate. (B) Cross-sectional image of cell patterned substrate. (C) Filopodia extend along the top of ridges and bottom of grooves. Lamellipodia protrude into the grooves at the cell edge along the topographic patterns (bottom left) but bridge the grooves at the leading edge of the cell.

ridges the measured width of focal adhesions was intermediate between the widths found on 70 nm and 400 nm wide ridges. When the ridge width increased from 650 nm to 1900 nm, the measured width of the focal adhesions remained constant. However, on the wider ridges the variability in focal adhesion widths was higher. On smooth SiOx, the focal adhesion widths were larger on average than on any of the patterned substrates (Fig. 14). The variability in focal adhesion widths was high on these substrates and very large loci of vinculin staining seemed to arise from coalescence of multiple focal adhesions. The measured widths of focal adhesions were larger than the ridge widths on ridges up to 650 nm wide, but remained smaller than the pattern pitches. On the 70 nm wide ridges on a 400 nm pitch, we occasionally observed focal adhesions that were not aligned with the grooves and ridges and spanned several grooves and ridges.

## Discussion

Human corneal epithelial cells elongated and aligned along 70 nm wide ridges. To our knowledge, these are the smallest features reported to induce contact guidance. Furthermore, the percentage of cells that aligned with the 70 nm wide ridges, on a 400 nm pitch, was similar to the percentage of cells aligned along ridges an order of magnitude wider.

Human corneal epithelial cell alignment along micrometer- and nanometer-sized grooves and ridges does not require the formation and alignment of focal adhesions and stress fibers along the topographic features. Focal adhesions and associated actin stress fibers were observed only sporadically in aligned cells, after 12 hours of incubation, on all patterned substrates. There are no previous reports on the orientation of focal adhesions in epithelial cells cultured on topographically patterned substrates. Focal adhesion and microfilament alignment was observed in fibroblasts and macrophages aligned along micrometer-sized grooves and ridges (Britland et al., 1996; den Braber et al., 1998; Matsuzaka et al., 2000; Meyle et al., 1994; Walboomers et al., 1998) and was proposed to be the driving force for the observed contact guidance. The generation of tension by actin stress fibers is known to be
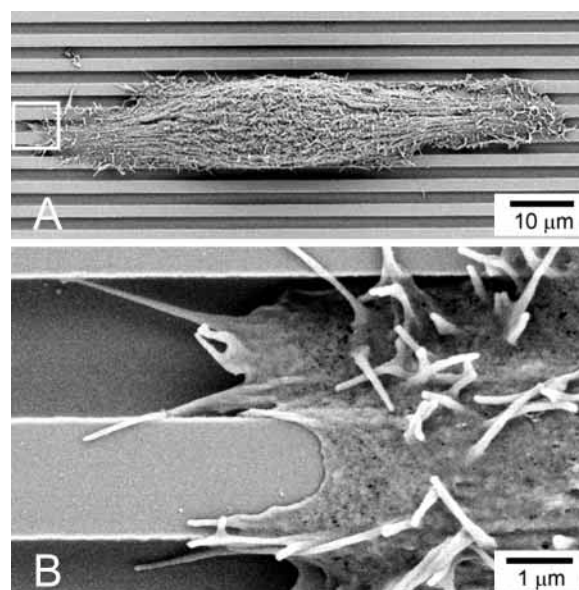


**Fig. 12.** SEM images of cells cultured on patterns with 4000 nm pitch. (A) Cell aligned along microstructured substrate. (B) At the cell edges perpendicular to the patterns, lamellipodia were able to adhere to the floor of the grooves on 2100 nm wide grooves.

necessary for the formation of focal adhesions (Chrzanowska-Wodnicka and Burridge, 1996). Nonetheless, fibroblasts have been reported to align along grooves and ridges before well-formed actin filaments were observed (Oakley and Brunette, 1993; Walboomers et al., 2000). Additionally, contact guidance, albeit delayed, has been observed to occur in the presence of poisons that disrupt the actin cytoskeleton in fibroblasts (Oakley and Brunette, 1995b; Oakley et al., 1997; Walboomers et al., 2000; Wojciak-Stothard et al., 1995a). We therefore conclude that focal adhesion and microfilament alignment is not a prerequisite for contact guidance.

Our results do not support a mechanism for contact guidance solely on the basis of the reaction of cells to surface

**Fig. 13.** Cells stained for actin (red), vinculin (green) and the nucleus (blue) as described in Materials and Methods. (A) Cell on a substrate with 600 nm deep grooves and 70 nm wide ridges on a 400 nm pitch. (B) Cell on a substrate with 600 nm deep grooves and 1900 nm ridges on a 4000 nm pitch. A reflection image of the substrates is included in the figure insets. (C) Cell on a smooth silicon oxide substrate.
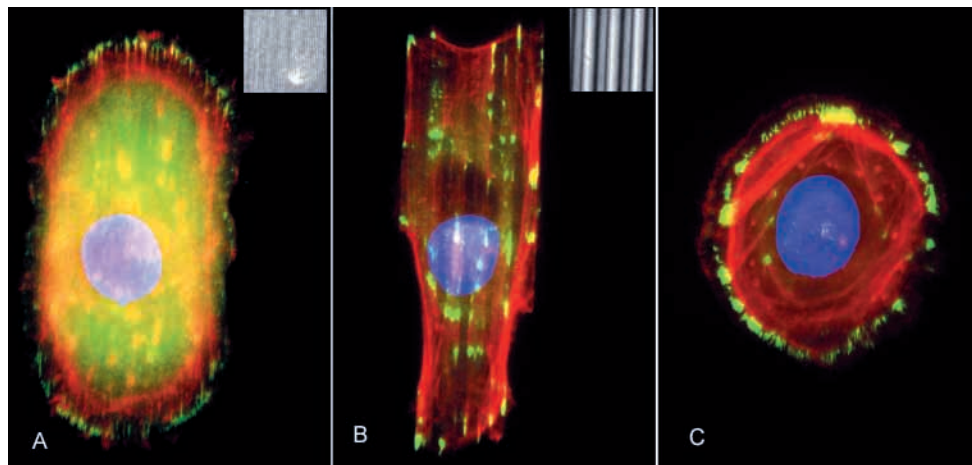
discontinuities. The number of discontinuities spanned by a single cell is ten times larger on substrates with feature pitches of 400 nm than when the pitch is 2000 nm. However, substrates with pitches ranging from 400 nm to 2000 nm yielded equivalent percentages of aligned cells. Actin and vinculin condensations along surface discontinuities have been described on macrophages (Wojciak-Stothard et al., 1995a), fibroblasts (Wojciak-Stothard et al., 1996) and epithelial cells (Oakley and Brunette, 1993; Oakley and Brunette, 1995a) cultured on micrometer-wide grooves and ridges. These were proposed to result from the mechanical interaction of the cell membrane with the ridge edges and were identified as the first step in the process of contact guidance in fibroblasts (Wojciak-Stothard et al., 1996; Wojciak-Stothard et al., 1995a). Furthermore, actin condensations along substrate discontinuities were still observed on cells treated with cytoskeletal poisons, offering an explanation for the observed contact guidance on these cells. We have seldom observed actin condensations along the ridge edges in aligned cells. When we did observe actin condensations they were usually continuous and located at the cell outline, unlike the condensations described previously (Wojciak-Stothard et al., 1996; Wojciak-Stothard et al., 1995a), which had a punctuate morphology. These differences may be ascribed to the use of different cell types. The percentage of aligned cells only decreased when the pitch was 4000 nm, on substrates with 600 nm deep grooves. Several studies report that the percentage of aligned cells is inversely proportional to ridge width (den Braber et al., 1996a; Walboomers et al., 1999a). For human corneal epithelial cells it appears that the ridge width of 1000 nm (2000 nm pitch) is the threshold below which this effect is not detected, for 600 nm deep grooves.

Only a subpopulation of cells elongated and aligned along the patterned topographies. Many of the remaining cells appeared rounded up when observed using SEM (data not shown). Live cell imaging confirmed that a subpopulation of cells did not spread and remained round for the duration of the experiment (until 12 hours after cell seeding). Therefore, the low percentage of cells aligned along the patterned substrates reflects in part the inability of a subpopulation of human corneal epithelial cells to spread on the silicon oxide surface. Consistent with this, the percentage of nonspread cells (defined as cells with elongation less than 1.3 and area less than 600

$\mu m^2$) was substantially larger on smooth or patterned silicon oxide surfaces than on TCPS (data not shown). In addition, the average areas of round cells were larger than the average areas of elongated cells (Figs 8 and 10). The chemical composition of the deposited layer of silicon oxide may therefore not be as favorable as TCPS for human corneal epithelial cell culture. Time-lapse microscopy also revealed that cells extended and retracted lamellipodia periodically and often acquired a round morphology after lamellipodial retraction, accounting for part of the population of round cells. By contrast, almost all NIH 3T3 fibroblasts cultured on similar patterned substrates aligned along the substrate features (data not shown). This is in agreement with the large percentages of fibroblasts that have been previously found to align along micrometer wide grooves and ridges.

Cell alignment was significantly greater on 600 nm deep than on 150 nm deep grooves, for pitches ranging from 400 nm to 2 μm. Although not explored in our studies, it is possible that the level of alignment we observed could be further increased by increasing groove depth. An increase in cell alignment with groove depth was observed in studies where the
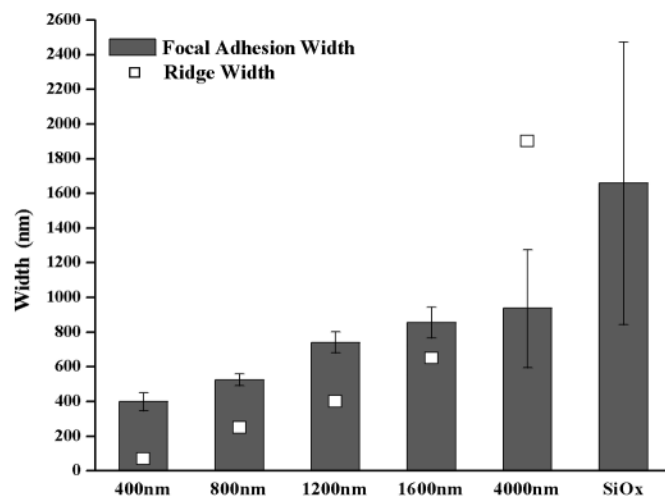


**Fig. 14.** Average focal adhesion widths for cells cultured on smooth or patterned silicon oxide substrates. The ridge width for each of the patterned substrates is indicated (open squares).

width of grooves and ridges was in the micrometer range and the groove depths were 0.5 μm or larger (Clark et al., 1990; Walboomers et al., 1999b). On grooves with nanoscale depths, cell alignment also correlated with groove depth, for both nanoscale (Clark et al., 1991) and micrometer-scale lateral feature dimensions (Wojciak-Stothard et al., 1996). Cells have been found increasingly able to descend into the grooves and form focal adhesions on the floor of the grooves as the ridge width was increased and the groove depth decreased (Walboomers et al., 1998; Walboomers et al., 1999a). On 1 μm or 2 μm wide grooves, cells have rarely been reported to protrude into the grooves (Walboomers et al., 1999a) and therefore most adhesions were observed to occur on the ridge (Matsuzaka et al., 2000; Meyle et al., 1994; van Kooten and von Recum, 1999). We observed that lamellipodia at the leading and trailing edges of the cells did not descend into the grooves, for groove widths ranging from 950 nm (2000 nm pitch) down to 330 nm (400 nm pitch), on both 150 nm and 600 nm deep grooves. On 2100 nm wide grooves lamellipodia frequently conformed to the grooves on 150 nm deep grooves and were sometimes able to contact the floor of the grooves on 600 nm deep grooves. Filopodia were able to adhere to the grooves and ridges and were frequently aligned by the topographic features. We therefore propose that filopodia play an important role in the capacity of cells to perceive the depth of topographic features. Fibroblasts were reported to produce more Fn mRNA on grooved substrates than on smooth substrates (Chou et al., 1995). It was proposed that this response depends on groove depth and results from an attempt to fill the grooves and stabilize the areas of the cell surface that span the grooves (van Kooten and von Recum, 1999). However, thick protein deposits on the grooves have not been observed in sections using transmission electron microscopy (den Braber et al., 1998), and we have not detected them by cross sectional SEM. Unfavorable surface chemistry for cell adhesion at the bottom of the grooves compared with the top of the ridges has been proposed to account for the inability of cells to contact the floor of the grooves (Matsuzaka et al., 2000; Walboomers et al., 1999b). We averted this problem by coating the features with silicon oxide, obtaining a uniform surface chemistry. An argument can be raised that differential diffusion on the shallow and deep grooves accounts for the dependence of alignment on groove depth. However, recent research suggests that increased corneal epithelial cell migration on porous filters is independent of diffusional limitations but attributable to the topographic features themselves (Dalton et al., 2001a).

Cells cultured in the presence of serum aligned to the substrate topographic patterns to a greater degree than cells cultured on the same basal medium not supplemented with serum. Serum contains adhesive and nonadhesive proteins that adsorb onto the surface before cells adhere. Therefore, the chemistry of the surface that cells encounter during initial adhesion is vastly different when serum is present from when no serum has been added to the medium (Franco et al., 2000). Formation of focal adhesions depends on the presence of ECM proteins on the substrate (Burridge and Chrzanowska-Wodnicka, 1996). However, we found that some cells in serum-free medium form focal adhesions after 12 hours of incubation, suggesting that these cells deposited extracellular matrix proteins during this period. Serum also provides cells with an array of growth factors that initiate cell-signaling pathways on binding to cell-surface receptors. Some of these pathways are interrelated to pathways stimulated by cell attachment to the substrate and may therefore act in concert to amplify the effect of the topographical stimuli. Interestingly, in the absence of serum, the average cell area was similar on smooth silicon oxide and on TCPS. By contrast, the average cell area in the presence of serum was approximately 50% larger on TCPS than on silicon oxide. Supplementing the cell culture medium with serum reduced the percentage of nonspread cells on TCPS by more than 50% compared to serum-free medium but had no effect on the percentage of nonspread cells on silicon oxide. This suggests that TCPS supports a layer of adsorbed protein from the serum with more favorable compositions and/or conformations for cell spreading than silicon oxide does.

Geometrical constraints imposed by the substrate dictated the focal adhesion architecture. SEM revealed that the cell membrane bridges the grooves, confining integrin occupancy to the top of the ridges. The width of focal adhesions observed on cells cultured on substrates with ridge widths larger than 400 nm was relatively constant. When the width of the ridges was reduced to 70 nm, smaller than the reported width of mature focal adhesions (250-500 nm) (Ohara and Buck, 1979) the average width of focal adhesions decreased. The measured average focal adhesion width on 70 nm wide ridges (400 nm) is consistent with the value expected when an object less than 100 nm wide is imaged by fluorescence microscopy (Kozubek, 2001). We therefore suggest that these focal adhesions are confined to the top of one ridge. Interestingly, we have occasionally observed focal adhesions that were not aligned with the topographic features and spanned more than one pattern pitch. Aggregation of ligand-bound integrins on these focal adhesions was not uniform but was restricted to the ridges. Therefore, ligand spacings of at least 330 nm were presented to the cells. Substrates with well-defined topographic features offer the opportunity to investigate minimum ligand spacing and clustering required for the formation of focal adhesions. They offer the advantage of providing well-defined spacings and eliminating the possibility of haphazard ligand clustering relative to smooth substrates coated with integrin binding ligands (Maheshwari et al., 2000; Massia and Hubbell, 1991).

Our results are consistent with a mechanism for contact guidance involving anisotropic force generation by lamellipodia and filopodia. As described above, we found that cells were able to align along the substrate features without the alignment of focal adhesions and stress fibers. The formation of focal adhesions and actin stress fibers is not necessary for cell spreading (Cox and Huttenlocher, 1998; Dunn and Brown, 1986; Greenwood and Murphy-Ullrich, 1998). Cells must nevertheless exert a tractive force on the substrate via focal complexes formed in filopodia and lamellipodia (Dunn and Brown, 1986). It has previously been hypothesized that contact guidance results from filopodial propagation being halted or hindered when filopodia face the ridge wall (Dalton et al., 2001b). We found that filopodia that protruded from the sides of the cells were often bent at the point of contact with the substrate and were subsequently aligned with the grooves and ridges, preventing the generation of force in the direction perpendicular to the ridges. Filopodia at the leading and trailing edges of cells were often extended along the top of the ridges or the floor of the grooves. Filopodial guidance by the

substrate features was more prevalent on the patterned topographies with the smaller pitches compared with the micrometer-wide grooves and ridges. To bridge a groove, cell protrusions must adhere to the top of a nearby ridge. The edges of lamellipodia were frequently seen to extend into the grooves, especially on the patterns with 400 nm pitch. Therefore, the failure of lamellipodia to reach adjacent ridges, becoming effectively trapped in the groove, may contribute to inhibition of lateral spreading. This effect was not observed on the widest and shallowest substrate features, 150 nm deep grooves on a 4000 nm pitch, where lamellipodia were able to conform to the topographic features. Consistent with this mechanism, live cell imaging showed that protrusions perpendicular to the patterns were not prohibited but were severely inhibited. Cell alignment resulted from anisotropic cell spreading as cells extended and retracted lamellipodia preferentially along the direction of the patterns.

## References

**Abrams, G. A., Goodman, S. L., Nealey, P. F., Franco, M. and Murphy, C. J.** (2000a). Nanoscale topography of the basement membrane underlying the corneal epithelium of the rhesus macaque. *Cell Tissue Res.* **299**, 39-46.

**Abrams, G. A., Schaus, S. S., Goodman, S. L., Nealey, P. F. and Murphy, C. J.** (2000b). Nanoscale topography of the corneal epithelial basement membrane and Descemet's membrane of the human. *Cornea* **19**, 57-64.

**Abrams, G. A., Bentley, E., Nealey, P. F. and Murphy, C. J.** (2002). Electron microscopy of the canine corneal basement membranes. *Cells Tissues Organs* **170**, 251-257.

**Britland, S., Morgan, H., Wojiak-Stodart, B., Riehle, M., Curtis, A. and Wilkinson, C.** (1996). Synergistic and hierarchical adhesive and topographic guidance of BHK cells. *Exp. Cell Res.* **228**, 313-325.

**Burridge, K. and Chrzanowska-Wodnicka, M.** (1996). Focal adhesions, contractility, and signaling. *Annu. Rev. Cell Dev. Biol.* **12**, 463-519.

**Chou, L., Firth, J. D., Uitto, V.-J. and Brunette, D. M.** (1995). Substratum surface topography alters cell shape and regulates fibronectin mRNA level, mRNA stability, secretion and assembly in human fibroblasts. *J. Cell Sci.* **108**, 1563-1573.

**Chrzanowska-Wodnicka, M. and Burridge, K.** (1996). Rho-stimulated contractility drives the formation of stress fibers and focal adhesions. *J. Cell Biol.* **133**, 1403-1415.

**Clark, P., Connolly, P., Curtis, A. S., Dow, J. A. and Wilkinson, C. D.** (1990). Topographical control of cell behaviour: II. Multiple grooved substrata. *Development* **108**, 635-644.

**Clark, P., Connolly, P., Curtis, A. S. G., Dow, J. A. T. and Wilkinson, C. D. W.** (1991). Cell guidance by ultrafine topography in vitro. *J. Cell Sci.* **99**, 73-77.

**Cox, E. A. and Huttenlocher, A.** (1998). Regulation of integrin-mediated adhesion during cell migration. *Microsc. Res. Tech.* **43**, 412-419.

**Dalton, B. A., McFarland, G. A. and Steele, J. G.** (2001a). Stimulation of epithelial tissue migration by certain porous topographies is independent of fluid flux. *J. Biomed. Mater. Res.* **56**, 83-92.

**Dalton, B. A., Walboomers, X. F., Dziegielewski, M., Evans, M. D., Taylor, S., Jansen, J. A. and Steele, J. G.** (2001b). Modulation of epithelial tissue and cell migration by microgrooves. *J. Biomed. Mater. Res.* **56**, 195-207.

**den Braber, E. T., de Ruijter, J. E., Ginsel, L. A., von Recum, A. F. and Jansen, J. A.** (1995). Effect of parallel surface microgrooves and surface energy on cell growth. *J. Biomed. Mater. Res.* **29**, 511-518.

**den Braber, E. T., de Ruijter, J. E., Smits, H. T. J., Ginsel, L. A., von Recum, A. F. and Jansen, J. A.** (1996a). Quantitative analysis of cell proliferation and orientation on substrata with uniform parallel surface micro-grooves. *Biomaterials* **17**, 1093-1099.

**den Braber, E. T., de Ruijter, J. E., Smits, H. T. J., Ginsel, L. A., von Recum, A. F. and Jansen, J. A.** (1996b). Quantitative analysis of fibroblast morphology on microgrooved surfaces with various groove and ridge dimensions. *Biomaterials* **17**, 2037-2044.

**den Braber, E. T., de Ruijter, J. E., Ginsel, L. A., von Recum, A. F. and Jansen, J. A.** (1998). Orientation of ECM protein deposition, fibroblast cytoskeleton, and attachment complex components on silicone microgrooved surfaces. *J. Biomed. Mater. Res.* **40**, 291-300.

**Dunn, G. A. and Brown, A. F.** (1986). Alignment of fibroblasts on grooved surfaces described by a simple geometric transformation. *J. Cell Sci.* **83**, 313-340.

**Flemming, R. G., Murphy, C. J., Abrams, G. A., Goodman, S. L. and Nealey, P. F.** (1999). Effects of synthetic micro- and nano-structured surfaces on cell behavior. *Biomaterials* **20**, 573-588.

**Franco, M., Nealey, P. F., Campbell, S., Teixeira, A. I. and Murphy, C. J.** (2000). Adhesion and proliferation of corneal epithelial cells on self-assembled monolayers. *J. Biomed. Mater. Res.* **52**, 261-269.

**Greenwood, J. A. and Murphy-Ullrich, J. E.** (1998). Signaling of de-adhesion in cellular regulation and motility. *Microsc. Res. Tech.* **43**, 420-432.

**Hironaka, K., Makino, H., Yamasaki, Y. and Ota, Z.** (1993). Renal basement membranes by ultrahigh resolution scanning electron microscopy. *Kidney Int.* **43**, 334-345.

**Inoue, S.** (1994). Basic structure of basement membranes is a fine network of "cords," irregular anastomosing strands. *Microsc. Res. Tech.* **28**, 29-47.

**Kozubek, M.** (2001). Theoretical versus experimental resolution in optical microscopy. *Microsc. Res. Tech.* **53**, 157-166.

**Kubosawa, H. and Kondo, Y.** (1994). Quick-freeze, deep-etch studies of renal basement membranes. *Microsc. Res. Tech.* **28**, 2-12.

**Maheshwari, G., Brown, G., Lauffenburger, D. A., Wells, A. and Griffith, L. G.** (2000). Cell adhesion and motility depend on nanoscale RGD clustering. *J. Cell Sci.* **113**, 1677-1686.

**Massia, S. P. and Hubbell, J. A.** (1991). An RGD spacing of 440 nm is sufficient for integrin alpha V beta 3-mediated fibroblast spreading and 140 nm for focal contact and stress fiber formation. *J. Cell Biol.* **114**, 1089-1100.

**Matsuzaka, K., Walboomers, F., de Ruijter, A. and Jansen, J. A.** (2000). Effect of microgrooved poly-l-lactic (PLA) surfaces on proliferation, cytoskeletal organization, and mineralized matrix formation of rat bone marow cells. *Clin. Oral Implants Res.* **11**, 325-333.

**Merker, H. J.** (1994). Morphology of the basement membrane. *Microsc. Res. Tech.* **28**, 95-124.

**Meyle, J., Gultig, K., Brich, M., Hammerle, H. and Nisch, W.** (1994). Contact guidance of fibroblasts on biomaterial surfaces. *J. Mater. Sci. Mater. Med.* **5**, 463-466.

**Oakley, C. and Brunette, D. M.** (1993). The sequence of alignment of microtubules, focal contacts and actin filaments in fibroblasts spreading on smooth and grooved titanium substrata. *J. Cell Sci.* **106**, 343-354.

**Oakley, C. and Brunette, D. M.** (1995a). Response of single, pairs, and clusters of epithelial cells to substratum topography. *Biochem. Cell Biol.* **73**, 473-489.

**Oakley, C. and Brunette, D. M.** (1995b). Topographic compensation: guidance and directed locomotion of fibroblasts on grooved micromachined substrata in the absence of microtubules. *Cell Motil. Cytoskel.* **31**, 45-58.

**Oakley, C., Jaeger, A. F. and Brunette, D. M.** (1997). Sensitivity of fibroblasts and their cytoskeletons to substratum topographies: topographic guidance and topographic compensayion by micromachined grooves of different dimensions. *Exp. Cell Res.* **234**, 413-424.

**Ohara, P. T. and Buck, R. C.** (1979). Contact guidance in vitro: a light, transmission, and scanning electron microscopic study. *Exp. Cell Res.* **121**, 235-249.

**Riveline, D., Zamir, E., Balaban, N. Q., Schwarz, U. S., Ishizaki, T., Narumiya, S., Kam, Z., Geiger, B. and Bershadsky, A. D.** (2001). Focal contacts as mechanosensors: externally applied local mechanical force induces growth of focal contacts by an mDia1-dependent and ROCK-independent mechanism. *J. Cell Biol.* **153**, 1175-1186.

**Ruben, G. C. and Yurchenco, P. D.** (1994). High resolution platinum-carbon replication of freeze-dried basement membrane. *Microsc. Res. Tech.* **28**, 13-28.

**Shirato, I., Tomino, Y., Koide, H. and Sakai, T.** (1991). Fine structure of the glomerular basement membrane of the rat kidney visualized by high-resolution scanning electron microscopy. *Cell Tissue Res.* **266**, 1-10.

**van Kooten, T. G., Whitesides, J. F. and von Recum, A. F.** (1998). Influence of silicone (PDMS) surface texture on human skin fibroblast proliferation as dtermined by cell cycle analysis. *J. Biomed. Mater. Res.* **43**, 1-14.

**van Kooten, T. G. and von Recum, A. F.** (1999). Cell adhesion to textured silicon surfaces: The influence of time of adhesion and texture on focal contact and fibronectin fibril formation. *Tissue Eng.* **5**, 223-240.

**von Recum, A. F. and van Kooten, T. G.** (1995). The influence of micro-topography on cellular response and the implications for silicone implants. *J. Biomater. Sci. Polym. Ed.* **7**, 181-198.

**Walboomers, X. F., Croes, H. J., Ginsel, L. A. and Jansen, J. A.** (1998). Growth behavior of fibroblasts on microgrooved polystyrene. *Biomaterials* **19**, 1861-1868.

**Walboomers, X. F., Croes, H. J. E., Gensel, L. A. and Jansen, J. A.** (1999a). Contact guidance of rat fibroblasts on various implant materials. *J. Biomed. Mater. Res.* **47**, 204-212.

**Walboomers, X. F., Monaghan, W., Curtis, A. S. G. and Jansen, J. A.** (1999b). Attachment of fibroblasts on smooth and microgrooved polystyrene. *J. Biomed. Mater. Res.* **46**, 212-220.

**Walboomers, X. F., Ginsel, L. A. and Jansen, J. A.** (2000). Early spreading events of fibroblasts on microgrooved substrates. *J. Biomed. Mater. Res.* **51**, 529-534.

**Webb, A., Clark, P., Skepper, J., Compston, A. and Wood, A.** (1995). Guidance of oligodendrocytes and their progenitors by substratum topography. *J. Cell Sci.* **108**, 2747-2760.

**Wojciak-Stothard, B., Curtis, A. S. G., Monaghan, W., McGrath, M., Sommer, I.. and Wilkinson, C. D. W.** (1995a). Role of the cytoskeleton in the reaction of fibroblasts to multiple grooved substrata. *Cell Motil. Cytoskeleton* **31**, 147-158.

**Wojciak-Stothard, B., Madeja, Z., Korohoda, W., Curtis, A. and Wilkinson, C.** (1995b). Activation of macrophage-like cells by multiple grooved substrata. Topographical control of cell behavior. *Cell Biol. Int.* **19**, 485-490.

**Wojciak-Stothard, B., Curtis, A., Monaghan, W., MacDonald, K. and Wilkinson, C.** (1996). Guidance and activation of murine macrophages by nanometric scale topography. *Exp. Cell Res.* **223**, 426-435.

**Yamasaki, Y., Makino, H. and Ota, Z.** (1994). Meshwork structures in bovine glomerular and tubular basement membrane as revealed by ultra-high-resolution scanning electron microscopy. *Nephron* **66**, 189-199.